3D Human Face Reconstruction Using a Hybrid of Photometric Stereo and Independent Component Analysis

[1]*Cheng-Jian Lin, [2]Shyi-Shiun Kuo, [1]Hsueh-Yi Lin, [2]Shye-Chorng Kuo and [1]Cheng-Yi Yu

Abstract

In this paper, we propose an improved photometric stereo scheme based on the Lambertian reflectance model and the constrained independent component analysis (cICA) method. When we obtain an object's surface normal vector on each point of an image using the ICA model to reconstruct 3D shapes, we find that the x-axis, y-axis and z-axis values of the normal vector's coordinates are not arranged in turn. Thus, we use the cICA method to solve the problem. We obtain the correct normal vector's sequence form surface, and use a method for enforcing integrability to reconstruct 3D objects. We tested our algorithm on synthetically generated images for the reconstruction of object surfaces and on a number of real images captured from the Yale Face Database B. The experimental results demonstrate that the proposed cICA method is better than some existing approaches.

Keywords: Photometric stereo, independent component analysis, face reconstruction.

1. Introduction

One of the approaches to computer vision is the photometric stereo approach for surface reconstruction. This approach is able to estimate local surface orientation by using several images of the same surface taken from the same viewpoint but under illuminations from different directions. It was first introduced by R. J. Woodham [1], who based it on the Lambertian reflectance model. It has received wide attention, and several efforts have been made to improve its recovery performance [2]-[18].

**Corresponding Author: Cheng-Jian Lin (E-mail:cjlin@ncut.edu.tw).*
[1]Department of Computer Science and Information Engineering,National Chi-Yi University of Technology, Taichung City 411, Taiwan.
[2]Department of Multimedia Animation and Application, Nankai University of Technology, Nantou County 542, Taiwan

The main limitation of the classical photometric stereo approach is that the light source positions must be accurately known. This necessitates a fixed, calibrated lighting rig. Hence, an improved photometric stereo method for estimating the surface normal and the surface reflectance of objects without a priori knowledge of the light source direction or the light source intensity was proposed by Hayakawa [3]. Hayakawa's method uses the singular-value decomposition (SVD) method to factorize an image data matrix of three different illuminations into a surface reflectance matrix and a light source matrix based on the Lambertian model. However, Hayakawa still uses one of the two added constraints for finding the linear transformation between the surface reflectance matrix and the light source matrix. McGunnigle [4] introduced a simple photometric stereo scheme, which only considered a Lambertian reflectance model, where the self and cast shadows, as well as the inter-reflections, were ignored. Three images at a tilt angle of 90° increments were captured. McGunnigle suggested using his method as a first estimate for an iterative procedure.

Belhumeur et al. [11] showed that a generalized bas-relief transformation is a transformation of both the surface shape and the surface albedo for an arbitrary Lambertian surface. The set of images of an object in a fixed post but under all possible illumination conditions is a convex cone (illumination cone) in the space of images. When the surface reflectance can be approximated as Lambertian, this illumination cone can be constructed from a handful of images acquired under variable lighting. Belhumeur et al. used as few as seven images of a face in a fixed pose, but they also used illumination by point light sources at varying and unknown positions to estimate the surface geometry of the face images and albedo which map up to a generalized bas-relief transformation. Despite their announced success of their method under unknown light source directions, the estimation of the surface

methods still required assistance using some added constraints or more images. Thus C.T. Lin, W.C. Cheng, and S.F. Liang proposed a Neural Network Based Adaptive Hybrid Reflectance Model [6]. In a neural network's training process, we obtain a surface normal vector without knowing the source directions in advance. Because of the neural network's light directions at the hidden level, those light directions nearly approach real light directions. This should affect the accuracy of a reconstructed model. C.T. Lin et al. also proposed a novel ICA-based photometric stereo approach based on a non-Lambertian model [7]. The goal of the ICA model is to separate the independent component of a surface normal on each point of an image. But the ICA model still has the problem of the x-axis, y-axis and z-axis values of the separated normal vector not being arranged in turn.

In this paper, we propose a technique that uses the constrained independent components analysis (cICA) model [20]-[25]. It is a supervised ICA model which may make the outputs of a normal vector's coordinate values arranged in turn. The 3D surface model is reconstructed from the surface normal on each point of an image, obtained by the cICA technique, and used a method for enforcing integrability [19]. The reason for those methods is easy to implement.

The rest of this paper is organized as follows Section 2 describes the Lambertian model. The details of the proposed cICA-based reflectance model and its derivations are presented in Section 3. We present the acquisition of the surface normal of objects using the cICA model in Section 4. In Section 5, we use the enforcing integrability approach to obtain detailed information for reconstructing the surface of an object using its normal vectors. Extensive experiments are performed to evaluate the performance of the proposed approach; some of the results are presented in Section 6. Conclusions are given in the last section.

2. The lambertian model

Lambertian surface mean angle can get the same surface of illumination. The illumination of observing the factor is only involved in the direction of the light source. Suppose that the recovery of a surface shape denoted by z(x, y) from shaded images, depends upon the systematic variation of the image brightness with the surface orientation, where z is the depth field, and x and y form the 2D grid over the domain D of the image plane. Then the Lambertian reflectance model used to represent a surface illuminated by a single point light source is written as:

$$R\left(\mathbf{n}_{x,y}, \alpha_{x,y}\right) = L\,\alpha_{x,y}\ \mathbf{s}^{T}\mathbf{n}_{x,y}, \forall x, y \in D, \qquad (1)$$

where $R(\cdot)$ is the diffuse component intensity, $\alpha_{x,y}$ is the diffuse albedo at location (x, y) of the surface, s is a column vector indicating the direction of the point light, and L is the light strength. The surface normal at location (x, y), denoted by $\mathbf{n}(x, y)$, can be represented as

$$n_{x,y} = \frac{\left[-p_{x,y} - q_{x,y}\ 1\right]^{T}}{\sqrt{p_{x,y}^{2} + q_{x,y}^{2} + 1}} \qquad (2)$$

where $p(x, y) = \partial z(x, y)/\partial x$ and $q(x, y) = \partial z(x, y)/\partial y$ are the surface gradients [1].

The Lambertian model describes a diffuse reflection surface, which involves light being reflected on average from all directions after modulation by the surface reflection rate. It is a useful model in the field of computer vision

3. The constrained ICA model

ICA is a technique that transforms a multivariate random signal into a signal having components that are mutually independent in the complete statistical sense [20]. Let the time-varying observed signal be $\mathbf{x}=(x_1, x_2, \ldots, x_m)^T$, and the desired signal consisting of independent components (ICs) be $s=(s_1, s_2, \ldots, s_n)^T$. The classical ICA assumes that the signal x is an instantaneous linear mixture of Ics, or independent sources s_i, i=1, 2, .. m. Therefore, x=As, where the matrix A of size $n \times m$ represents the linear memoryless mixing channels.

The goal of the ICA is to obtain a $m \times n$ demixing matrix W to recover all the ICs of the observed signal. y=(y1, y2, …,ym)T is given by y=Wx. For simplicity, in this paper, we address the case of a complete ICA, in which $n = m$.

The following is used to solve the surface normal **n**(*x*,*y*) for all and in Eq. (1) from 2D image intensity. Since the **n**(*x*,*y*) vector is a 3 1 column vector, we would need at least three images under illumination from light coming from different directions. If the location of the light sources were given, we could solve the normal vector on surfaces at every location (x, y). We know that the problem of solving Eq. (1) is a separation blind problem. Our previous research used the ICA model to solve the problem of finding the surface normal on each point of an image. But in the ICA model, it is easy to see that the following ambiguities exist [20]: 1) We cannot determine the variances (energies) of the independent components; and 2) We cannot determine the order of the independent components. We will generally discover that finding the surface normal vector involves the two problems. For those reasons, we use a constrained learning adaptation algorithm (cICA) based on image intensities to handle these ambiguities.

The cICA algorithm described in [21] brings in the use of a constraint which is used to obtain an output that is statistically independent of other sources and is closest to a reference signal r(t). This constraining signal need not be a perfect match but it should be enough to point the algorithm in the direction of a particular IC spanning the measurement space. The closeness constraint can be written as

$$g(w) = \varepsilon(w) - \xi \leq 0 \qquad (3)$$

where w denotes a single demixing weight vector such that $y=w^T$; $\varepsilon(w)$ represents the closeness between the estimated output y and the reference r, and ξ represents some closeness threshold. The measure of closeness can take any form, such as mean squared-error (MSE) or correlation, or any other suitable closeness measure. In our implementation of the algorithm, we use correlation as a measure of closeness such that $g(w)$ becomes

$$g(w) = \xi - E\{r(w^T v)\} \leq 0 \qquad (4)$$

where ξ now becomes the threshold that defines the lower bound of the optimum correlation.

With the constraint in place, the cICA problem is modeled as follows:

Maximize: $(w) = \rho[E\{G(w^T v)\} - E\{G(V)\}]^2$,

Subject to:

$$g(w) \leq 0,\ h(w)=E\{y^2\}-1=0 \text{ and } E\{r^2\}-1=0, \qquad (5)$$

where f(w) denotes the one-unit ICA contrast function; g(w) is the closeness constraint; h(w) constrains the output y to having a unit variance; and the reference signal r is also constrained to having a unit variance. In [38], the problem of (5) is expressed as a constrained optimization problem which is solved through the use of an augmented Lagrangian function, where learning of the weights and the Lagrange parameters is achieved through a Newton-like learning process.

For example, the cICA algorithm was tested using a synthetic data set of four known sources were seen in Fig. 1(a), which had been used for ICA work. The sources were linearly mixed by a randomly generated mixing matrix, producing the dataset shown in Fig. 1(b). With this mixture of data, the cICA algorithm was run 100,000 times, each time with one of the five reference signals shown in Fig. 1(c) as a reference. The first four of these references were obtained from the sign of the four original sources, and these were purposely kept as coarse representations of the true sources. The fifth reference is a sine wave which has a frequency radically different than any of the original sources, allowing study of the algorithm's behavior given a "false" reference. Typical outputs of the algorithm are depicted in Fig. 1(d). Thus, if we want to find the surface normal vector on each point of an image, we can use the cICA model to find it.

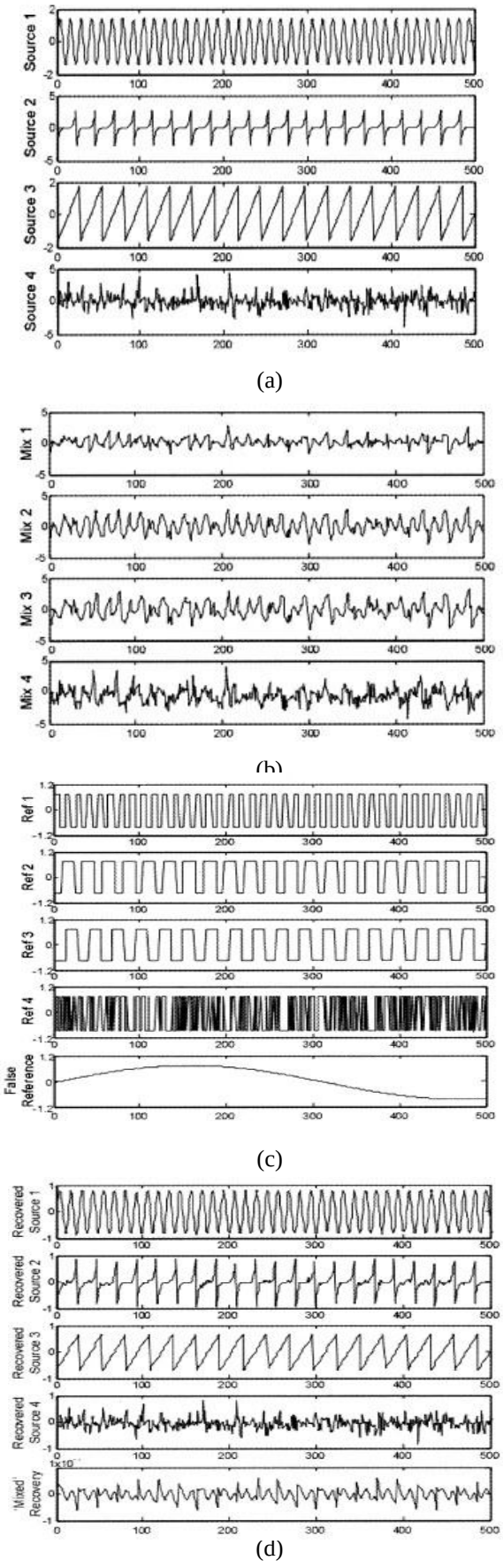

Figure 1: (a) The four underlying sources of the synthetic dataset. (b) The linearly mixing underlying sources shown in (a). (c) The different references used for executions of cICA on 4 channels of data in (b). The first four references are derived from the signs of the four underlying source and the fifth reference is a "false" reference. (d) Examples of each recovered source using only the references given in (c), the fifth recovered source shows a "mixture" of two underlying sources.

4. Determining the surface normal of objects using the cICA model

In this section, we will describe the method of applying the ICA model to estimate the normal vector $\mathbf{n}(x, y)$ on the object surface corresponding to each pixel in an image. Since the $\mathbf{n}(x, y)$ vector is a 3×1 column vector, we need at least three images under illumination from lights coming from different directions for the normal vector $\mathbf{n}(x, y)$ estimation. Hence, to reconstruct the 3D surface of an object using its images, we have to take three gray-value images under three different illuminants. Assuming an image contains T pixels in total, we can rearrange all the gray values of the three images into a 3×T matrix, with each row representing an image, and each column representing the gray values of a single pixel under three different illuminants. When this matrix is put into Eq. (1), and Eq. (1) is compared with $\mathbf{x} = \mathbf{As}$, we find that $\mathbf{s}$ is the $\mathbf{n}(x, y)$ vector.

Using the ICA decomposition, we rewrite equation (1) in matrix form as

$$\mathbf{x}(i) = \mathbf{As}(i) = \alpha(i)\hat{\mathbf{A}}\,\hat{\mathbf{n}}(i), \qquad (6)$$

where $\hat{\mathbf{A}} = [a_1, a_2, a_3]^T = \hat{W}^{-1}$ is the matrix depending on the lighting and viewing directions and has unit length; $\hat{\mathbf{n}}(t)$ is the estimated normal vector corresponding to the tth pixel, i = 1, 2, …, T; and (i) is the albedo of the ith pixel. However, the decomposition in Eq. (6) is not unique. If there is an invertible matrix G, which satisfies

$$A=\hat{\mathbf{A}}G \text{ and } n(i)=G^{-1}\hat{\mathbf{n}}(i), \qquad (7)$$

where A is the true matrix depending on the lighting and viewing directions of the images, and **n**(*i*) is the normal vector of the ith pixel in the standard XYZ coordinates, then the linear ambiguity belongs to the subset of GBR [11]-[13]. On the one hand, according to Georghiades's [13] studies, if the surface of an object is seen under variable light directions, but with a fixed viewpoint, then the linear ambiguity can be reduced to three GBR parameters. As far as the surface normal vectors are concerned, we can only recover $\mathrm{n} \cong G^{-1}\hat{\mathbf{n}}$, and

$$G^{-1} = \frac{1}{g_3}\begin{bmatrix} g_3 & 0 & 0 \\ 0 & g_3 & 0 \\ -g_1 & -g_2 & 1 \end{bmatrix} \quad (8)$$

where g_i are the three GBR parameters. On the other hand, the three light sources corresponding to the three images do not lie in the same plane (non-coplanar); therefore, the columns of matrix A are linearly independent. In addition, using the ICA decomposition in Eq. (6), we can obtain an independent basis matrix $\hat{\mathbf{A}}$; thus the ambiguity can further be denoted by a diagonal matrix, i.e., g1 = 0 and g2 = 0. The relation, then, between the normals in the standard XYZ coordinates and those in the independent coordinates system differs only by the g3 factor. For the performance evaluation of 3D image reconstruction, both estimated surfaces and synthetic surfaces are normalized within the interval [0, 1]. Therefore, the influence of the g3 factor on the estimated 3D surface can be removed.

5. 3D surface reconstruction from the surface normal using the method for enforcing integrability

In this section, we discuss using the method for enforcing integrability to obtain detailed information for reconstructing the surface of an object using its normal vectors. This approach was proposed by R. T. Frankot and R. Chellappa [19].

Suppose that we represent the surface by the functions so that

$$\mathrm{z(x,y)} = \sum_{\boldsymbol{\omega}\in\Omega} c(\boldsymbol{\omega})\emptyset(x,y,\boldsymbol{\omega}) \quad (9)$$

where $\boldsymbol{\omega} = (u, v)$ is a two-dimensional index, Ω is a finite set of indexes, and the members of $\{\emptyset(\mathrm{x,y},\boldsymbol{\omega})\}$ are not necessarily mutually orthogonal. We choose the discrete cosine basis so that $\{\mathrm{c}(\boldsymbol{\omega})\}$ is exactly the full set of discrete cosine transform (DCT) coefficients of *z(x, y)*. Since the partial derivatives of the basis functions, $\emptyset_x(x,y,\boldsymbol{\omega})$ and $\emptyset_x(x,y,\boldsymbol{\omega})$ are integrable, the partial derivatives of *z(x, y)* are guaranteed to be integrable as well; that is, $z_{xy}(x,y) = z_{yx}(x,y)$. Note that the partial derivatives of *z(x, y)* can also be expressed in terms of this expansion, giving

$$z_x(\mathrm{x,y}) = \sum_{\boldsymbol{\omega}\in\Omega} c(\boldsymbol{\omega})\emptyset_x(x,y,\boldsymbol{\omega}) \quad (10)$$

$$\mathrm{z}_y(\mathrm{x,y}) = \sum_{\boldsymbol{\omega}\in\Omega} c(\boldsymbol{\omega})\emptyset_y(x,y,\boldsymbol{\omega}) \quad (11)$$

where $\emptyset_x(x,y,\boldsymbol{\omega}) = \partial\emptyset(\cdot)/\partial\mathrm{x}$ and $\emptyset_y(x,y,\boldsymbol{\omega}) = \partial\emptyset(\cdot)/\partial y$.

Suppose we now have the possibly non-integrable estimate **n**(*x,y*) from which we can easily deduce from Eq. (2) the possibly non-integrable partial derivatives $\hat{z}_x(\mathrm{x,y})$ and $\hat{z}_y(\mathrm{x,y})$. These partial derivatives can also be expressed as a series, giving

$$\hat{z}_x(\mathrm{x,y}) = \sum_{\boldsymbol{\omega}\in\Omega} \hat{c}_1(\boldsymbol{\omega})\emptyset_x(x,y,\boldsymbol{\omega}) \quad (12)$$

$$\hat{z}_y(\mathrm{x,y}) = \sum_{\boldsymbol{\omega}\in\Omega} \hat{c}_2(\boldsymbol{\omega})\emptyset_y(x,y,\boldsymbol{\omega}) \quad (13)$$

This method can find the expansion coefficients $c(\boldsymbol{\omega})$ given a possibly non-integrable estimate of surface slopes $\hat{z}_x(\mathrm{x,y})$ and $\hat{z}_y(\mathrm{x,y})$:

$$c(\boldsymbol{\omega}) = \frac{p_x(\boldsymbol{\omega})\hat{c}_1(\boldsymbol{\omega}) + p_y(\boldsymbol{\omega})\hat{c}_2(\boldsymbol{\omega})}{p_x(\boldsymbol{\omega}) + p_y(\boldsymbol{\omega})}, \quad \text{for } \boldsymbol{\omega} = (\mathrm{u,v}) \in \Omega \quad (14)$$

where

$$p_x(\boldsymbol{\omega})=\iint |\emptyset_x(x,y,\boldsymbol{\omega})|^2 dxdy \quad (15)$$

$$p_y(\boldsymbol{\omega})=\iint |\emptyset_y(x,y,\boldsymbol{\omega})|^2 dxdy \quad (16)$$

In the end, we can reconstruct an object's surface by implementing the inverse 2D DCT on the coefficient $c(\boldsymbol{\omega})$.

6. Experimental Results

We tested the algorithm on a number of real images from the Yale Face Database B [26] showing variability due to illumination. There are varying albedos in each point of the surface of the human faces (as shown in Fig. 2).

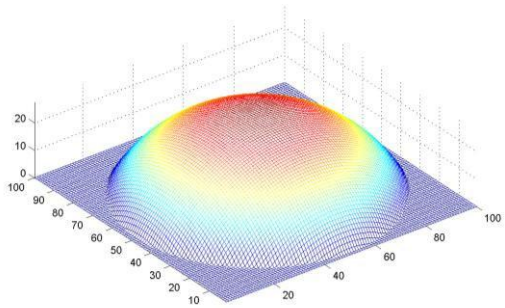

Figure 2: Synthetic sphere surface object.

First, we arbitrarily took from these test images the images of the same person who was photographed under three different light sources, as shown in the firstcolumnofFig. 4. We fed the normalized images into our algorithm. For the face surface reconstruction problem, the normal vectors of a sphere's surface were used as the reference values for the cICA model due to their similar structures. The true depth map of the synthetic sphere object is generated mathematically as

$$z(x,y)=\begin{cases} |\sqrt{r^2-x^2-y^2}| \text{ , if } x^2+y^2 \le r^2 \\ 0, \text{ otherwise} \end{cases} \quad (17)$$

where r=48, $0 < x, y \le 100$, and the center is located at (x, y)=(51, 51). The sphere object is shown in Fig. 2.Fig. 3 shows the normal vectors of a sphere's surface.

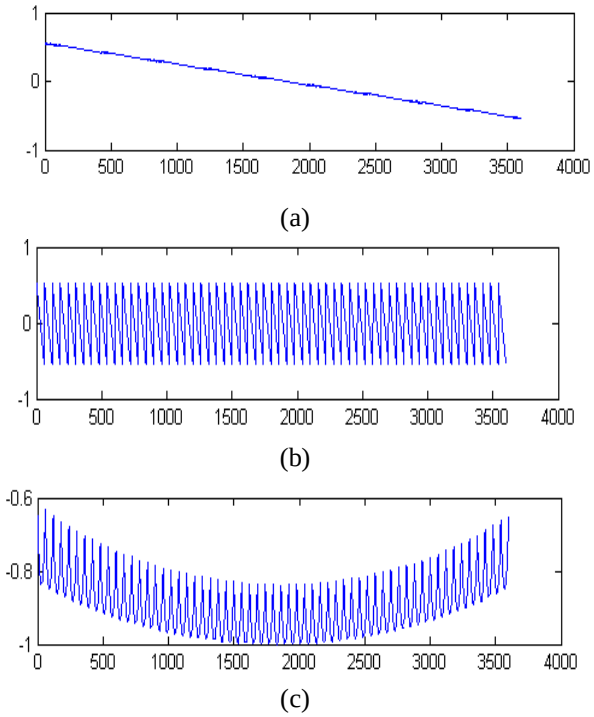

(a) (b) (c)

Figure 3: The normal vectors of a sphere's surface (a) the X-component, (b) the Y-component, and (c) the Z-component of the normal vectors.

After updating the parameters by several iterations, we obtained the normal vector of the surfaces of the human faces corresponding to each pixel in the image of the output nodes. The results are shown in the second column of Fig. 4, which give the X-component, the Y-component, and the Z-component of the surface normal vector in order.

(a) (b) (c) (d)

(e) (f)

Figure 4: (a)(c)(e) represent three training images with differ light source positions from Yale Face Database B in frontal. (b)(d)(f) represent surface normal corresponding to the three source images.

Figure 5 presents the results of the reconstructed 3D human face. Fig. 5(a) shows the surface albedo of the human face shown in Fig. 4. Fig. 5(b) shows the result from using our proposed algorithm. The reconstructed results find by using Georghiades's approach [12] and Hayakawa's approach [3] are shown in Fig. 5(c) and 5(d), respectively. The results clearly indicate that the performance of our proposed nonlinear reflectance model is better than that of Georghiades's approach and Hayakawa's approach. When the results obtained by using Georghiades's approach are compared with the results that find by using our proposed approach, the reconstructed surfaces resulting from our algorithm, taking into consideration the specular components, are obviously better in high-gradient areas, such as the nose. Hayakawa's approach required added constraints to be able to reconstruct a 3D model of a human face, which is similar to our approach. However, when the constraints were unavailable, it could not reconstruct a 3D model of a human face.

(a)

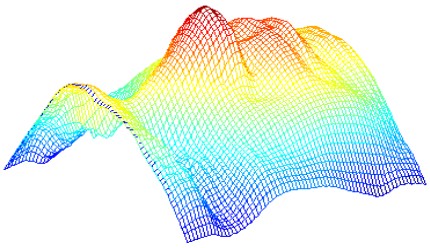

(b)

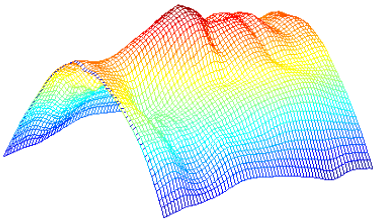

(c)

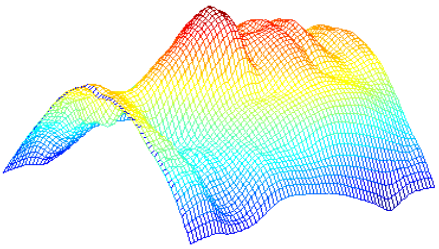

(d)

Figure 5: The surface albedo of human face in Fig. 4. The results of 3D model reconstruction by (b) our proposed algorithm, (c) Georghiades's approach in [12], and (d) Hayakawa's approach in [3].

7. Conclusions

The application of component analysis methods, such as ICA to surface normal vector analysis, has met with considerable success. However, when automated analysis techniques are required, the standard ICA algorithms prove to be less useful. Supervising the ICA solution by incorporating prior domain knowledge is logical, and it is in keeping with expert evaluation of neurophysiological signals, where for different evaluation purposes predetermined expectations of signal morphology and distribution are present. cICA as applied in this paper with temporal constraints results in a useful technique for the fast and efficient extraction of surface normal vectors from three surface reflection images. An important result derived from using the constrained cICA model for solving photometric stereo problems is desired output values and smoothing conditions are not needed. This allows for easier convergence and makes the system stable.

Performance comparisons of our proposed cICA-based photometric stereo approach with Georghiades's approach in [12] and Hayakawa's approach in [3] were made. We tested our proposed algorithm on human face images for the reconstruction of 3D human face surfaces. The results clearly indicate that the performances of our proposed approach are better than that of Georghiades's approach in [12] and Hayakawa's approach in [3]. All the experimental results showed that the performance of our proposed approach is better than those of the two existing photometric stereo methods.

References

[1] R. J. Woodham, "Photometric Method for Determining Surface Orientation from Multiple Images," Journal of Optical Engineering, Vol. 19, No. 1, 1980.

[2] K. M. Lee and C. J. Kuo, "Shape Reconstruction from Photometric Stereo," Journal of Optical Society of America: A, Vol. 10, No. 5, 1993.

[3] K. Hayakawa, "Photometric Stereo under a Light Source with Arbitrary Motion," Journal of the Optical Society of America: A, Vol. 11, No. 11, 1994.

[4] G. McGunnigle, "The Classification of Textured Surfaces under Varying Illuminant Direction," Ph.D. Thesis, Department of Computing and Electrical Engineering, Heriot-Watt University, Edinburgh, 1998.

[5] E. Angelopoulou and J. P. Williams, "Photometric Surface Analysis in a Triluminal Environment," Proceedings of IEEE International Conference on Computer Vision, 1999.

[6] C. T. Lin, W. C. Cheng, and S. F. Liang, "Neural-Network Base Adaptive Hybrid-Reflectance Model for 3-D Surface Reconstruction," IEEE Transactions On Neural Networks, Vol. 16, No. 6, pp1601-1615, November 2005.

[7] C. T. Lin, W. C. Cheng, and S. F. Liang, "A 3-D Surface Reconstruction Approach Based on Postnonlinear ICA Model," IEEE Transactions On Neural Networks, Vol. 16, No. 6, pp1638-1650, November 2005.

[8] C. Cho and H. Minanitani, "A New Photometric Method Using 3 Point Light Sources," IEICE Trans. Inf. & Syst. V.E76-D, No. 8, pp. 898-904, August 1993.

[9] G. Kay and T. Caelli, "Estimating the Parameters of an Illumination Model Using Photometric Stereo," Graphical Models and Image Processing, Vol. 57, No. 5, pp. 365-388, 1995.

[10] S. K. Nayar, K. Ikeuchi, and T. Kanade, "Determining Shape and Reflectance of Hybrid Surfaces by Photometric Sampling," IEEE Transactions on Robotics and Automation, Vol. 6, No. 4, pp. 418-431, 1990.

[11] P. N. Belhumeur, D. J. Kriegman, and A. L. Yuille, "The Bas-Belief Ambiguity," CVPR, pp. 1060-1066, 1997.

[12] S. Georghiades, P. N. Belhumeur, and D. J. Kriegman, "From Few to Many: Illumination Cone Models for Face Recognition under Variable Lighting and Pose," IEEE Trans. on Pattern Analysis and Machine Intelligence, Vol. 23, No. 6, pp. 643-660, June 2001.

[13] S. Georghiades, "Incorporating the Torrance and Sparrow Model of Reflectance in Uncalibrated Photometric Stereo," Proceedings of the Ninth IEEE International Conference on Computer Vision, 2003.

[14] H. D. Tagare and R. J. P. deFigueiredo, "Simulataeous Estimation of Shape and Reflectance Maps from Photometric Stereo," IEEE International Conference on Computer Vision, pp. 340-343, 1990.

[15] F. Solomon and K. Ikeuchi, "Extracting the Shape and Roughness of Specular Lobe Objects Using Four Light Photometric Stereo," IEEE Conference on Computer Vision and Pattern Recognition, pp. 466-471, 1992.

[16] H. Rushmeier, G. Taubin, and A. Gueziec, "Applying Shape from Lighting Variation to Bump Map Capture," In Eurographics Rendering Techniques'97, pp. 35-44, St. Etienne, France, June 1997.

[17] O. Drbohlav and A. Leonardis,"Detecting Shadows and Specularities by Moving Light,"Proceeding of Computer Vision Winter Workshop, Ljubljana, Slovenia, pp. 60-74, 1998.

[18] O. Drbohlav and R. Sara, "Specularities Reduce Ambiguity of Uncalibrated Photometric Stereo," Proceedings of the 7th European Conference on Computer Vision, Copenhagen, Denmark, 2002.

[19] R. T. Frankot and R. Chellappa, "A Method for Enforcing Integrability in Shape From Shading Algorithms," IEEE Trans. on Pattern Analysis and Machine Intelligence, Vol. 10, No. 4, pp. 439-451, July 1988.

[20] A. Hyvärinen, J. Karhunen, and E. Oja, Independent component analysis, John Wiley
& Sons, Inc., 2001.

[21] W. Lu and J. C. Rajapakse, "ICA with reference," in Proc. 3rd Int. Conf. Independent Component Analysis and Blind Signal Separation: ICA2001, pp. 120-125.

[22] C. J. James and O. J. Gibson, "Temporally constrained ICA: An Application to Artifact Rejection in Electromagnetic Brain Signal Analysis," IEEE Trans. on Biomedical Engineering, Vol. 50, No. 9, pp. 1108-1116, September 2003.

[23] W. Lu and J. C. Rajapakse, "Approach and Applications of Constraned ICA," IEEE Trans. on Neural Networks, Vol. 16, No. 1, pp. 203-212, January 2005.

[24] C. W. Hesse and C. J. James, "The FastICA Algorithm With Spatial Constraints," IEEE Signal Processing Letters, Vol. 12, No. 11, pp. 792-795, November 2005.

[25] S. A. Cruces-Alvarez, A. Cichocki, and S. Amari, "From blind signal extraction to blind instantaneous signal separation: criteria, algorithms, and stability," IEEE Trans. on Neural Networks, Vol. 15, No. 4, pp. 859-873, July 2004.

[26] The Yale Face Database B, Online available = http://cvc.yale.edu/projects/yalefacesB/yalefacesB.html.